Physics Letters B 738 (2014) 6–12

Contents lists available at ScienceDirect

Physics Letters B

www.elsevier.com/locate/physletb

Towards a data-driven analysis of hadronic light-by-light scattering

Gilberto Colangelo [a], Martin Hoferichter [a,*], Bastian Kubis [b], Massimiliano Procura [a], Peter Stoffer [a]

[a] Albert Einstein Center for Fundamental Physics, Institute for Theoretical Physics, Universität Bern, Sidlerstrasse 5, CH-3012 Bern, Switzerland
[b] Helmholtz-Institut für Strahlen- und Kernphysik (Theorie) and Bethe Center for Theoretical Physics, Universität Bonn, D-53115 Bonn, Germany

ARTICLE INFO

Article history:
Received 14 August 2014
Received in revised form 6 September 2014
Accepted 8 September 2014
Available online 16 September 2014
Editor: V. Metag

Keywords:
Dispersion relations
Anomalous magnetic moment of the muon
Compton scattering
Meson–meson interactions

ABSTRACT

The hadronic light-by-light contribution to the anomalous magnetic moment of the muon was recently analyzed in the framework of dispersion theory, providing a systematic formalism where all input quantities are expressed in terms of on-shell form factors and scattering amplitudes that are in principle accessible in experiment. We briefly review the main ideas behind this framework and discuss the various experimental ingredients needed for the evaluation of one- and two-pion intermediate states. In particular, we identify processes that in the absence of data for doubly-virtual pion–photon interactions can help constrain parameters in the dispersive reconstruction of the relevant input quantities, the pion transition form factor and the helicity partial waves for $\gamma^*\gamma^* \to \pi\pi$.

1. Introduction

The limiting factor in the accuracy of the Standard-Model prediction for the anomalous magnetic moment of the muon $a_\mu = (g-2)_\mu/2$ is control over hadronic uncertainties [1,2]. The leading hadronic contribution, hadronic vacuum polarization, is related to the total hadronic cross section in e^+e^- annihilation, so that the improvements necessary to compete with the projected accuracy of the FNAL and J-PARC experiments can be achieved with a dedicated e^+e^- program, see e.g. [3,4]. Owing to the complexity of the hadronic light-by-light (HLbL) tensor, a similar data-driven approach for the subleading[1] HLbL scattering contribution has only recently been suggested, and only for the leading hadronic channels [8]. In contrast to previous approaches [9–21], this formalism aims at providing a direct link between data and the HLbL contribution to a_μ. An alternative strategy to reduce model-dependence in HLbL relies on lattice QCD, see [22] for a first calculation.

The dispersive framework in [8] includes both the dominant pseudoscalar-pole contributions as well as two-meson intermediate states, thus covering the most important channels. In view of the fact that a data-driven approach for the HLbL contribution is substantially more involved than that for HVP, we present here an overview of this approach leaving aside all theoretical details, and emphasize which measurements can help constrain the required hadronic input. At present such an overview can only be obtained after studying several different theoretical papers. It is, however, essential that also experimentalists become fully aware that some measurements may have a substantial and model-independent impact on a better determination of the HLbL contribution to a_μ. This is the main aim of the present letter.

2. Theoretical framework

2.1. Dispersion relations

In dispersion theory the matrix element of interest is reconstructed from information on its analytic structure: residues of poles, discontinuities along cuts, and subtraction constants (representing singularities at infinity). In contrast to HVP, the complexity of the HLbL tensor prohibits the summation of all possible intermediate states into a single dispersion relation. Instead, one has to rely on an expansion in the mass of allowed intermediate states, justified by higher thresholds and phase-space suppression in the dispersive integrals. In this paper we concentrate on the lowest-lying intermediate states, the π^0 pole and $\pi\pi$ cuts, that illustrate the basic features of our dispersive approach and are expected to be most relevant numerically. We will comment on higher intermediate states in Section 4.

* Corresponding author.

[1] At this order also two-loop diagrams with insertions of hadronic vacuum polarization appear [5]. Even higher-order hadronic contributions have been recently considered in [6,7].

http://dx.doi.org/10.1016/j.physletb.2014.09.021

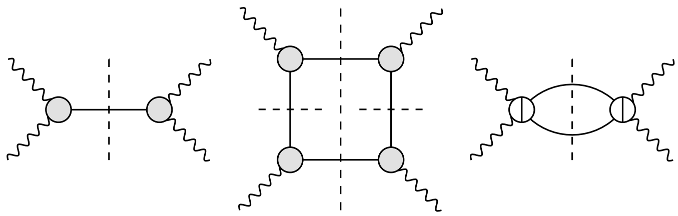

Fig. 1. Representative unitarity diagrams for the pion pole (left), the FsQED contribution (middle), and $\pi\pi$ rescattering (right). The gray blobs refer to the pertinent pion form factors, those with vertical line to the non-pole $\gamma^*\gamma^* \to \pi\pi$ amplitude. The dashed lines indicate the cutting of pion propagators. For more details see [8].

Given that each contribution to the HLbL tensor is uniquely defined by its analytic structure, it can be related unambiguously to a certain physical intermediate state. We decompose the HLbL tensor according to

$$\Pi_{\mu\nu\lambda\sigma} = \Pi^{\pi^0}_{\mu\nu\lambda\sigma} + \Pi^{\text{FsQED}}_{\mu\nu\lambda\sigma} + \Pi^{\pi\pi}_{\mu\nu\lambda\sigma} + \cdots, \tag{1}$$

where $\Pi^{\pi^0}_{\mu\nu\lambda\sigma}$ denotes the pion pole, $\Pi^{\text{FsQED}}_{\mu\nu\lambda\sigma}$ the amplitude in scalar QED with vertices dressed by the pion vector form factor F^V_π (FsQED), $\Pi^{\pi\pi}_{\mu\nu\lambda\sigma}$ includes the remaining $\pi\pi$ contribution, and the ellipsis higher intermediate states. Representative unitarity diagrams for each term are shown in Fig. 1.

The separation of the FsQED amplitude ensures that contributions with simultaneous cuts in two kinematic variables are correctly accounted for. In fact, $\Pi^{\text{FsQED}}_{\mu\nu\lambda\sigma}$ is completely fixed by the pion vector form factor, see [8] for details and explicit expressions. Since for this purpose F^V_π is known to sufficient accuracy experimentally, $\Pi^{\text{FsQED}}_{\mu\nu\lambda\sigma}$ is completely determined and we will concentrate on reviewing the central results for $\Pi^{\pi^0}_{\mu\nu\lambda\sigma}$ and $\Pi^{\pi\pi}_{\mu\nu\lambda\sigma}$ in the following.

2.2. Pion pole

The residue of the pion pole is determined by the pion transition form factor $\mathcal{F}_{\pi^0\gamma^*\gamma^*}(q_1^2, q_2^2)$. The corresponding contribution to a_μ follows from [17]

$$\begin{aligned}
a_\mu^{\pi^0} &= -e^6 \int \frac{d^4q_1}{(2\pi)^4} \int \frac{d^4q_2}{(2\pi)^4} \frac{1}{q_1^2 q_2^2 s Z_1 Z_2} \\
&\quad \times \bigg\{ \frac{\mathcal{F}_{\pi^0\gamma^*\gamma^*}(q_1^2, q_2^2)\mathcal{F}_{\pi^0\gamma^*\gamma^*}(s, 0)}{s - M_{\pi^0}^2} T_1^{\pi^0}(q_1, q_2; p) \\
&\quad + \frac{\mathcal{F}_{\pi^0\gamma^*\gamma^*}(s, q_2^2)\mathcal{F}_{\pi^0\gamma^*\gamma^*}(q_1^2, 0)}{q_1^2 - M_{\pi^0}^2} T_2^{\pi^0}(q_1, q_2; p) \bigg\}, \\
Z_1 &= (p + q_1)^2 - m^2, \qquad Z_2 = (p - q_2)^2 - m^2, \\
s &= (q_1 + q_2)^2,
\end{aligned} \tag{2}$$

where m denotes the mass of the muon, p its momentum, $e = \sqrt{4\pi\alpha}$ the electric charge, and the $T_i^{\pi^0}(q_1, q_2; p)$ are known kinematic functions.

It should be mentioned that the relation (2) only represents the π^0 pole, it does not, on its own, satisfy QCD short-distance constraints. As pointed out in [19], the pion pole as defined in (2) tends faster to zero for large q^2 than required by perturbative QCD due to the momentum dependence in the singly-virtual form factors. The correct high-energy behavior is only restored by the exchange of heavier pseudoscalar resonances, but the pion-pole contribution, by its strict dispersive definition, is unambiguously given as stated in (2).

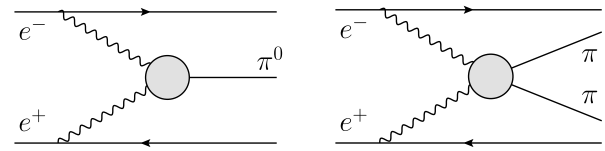

Fig. 2. $e^+e^- \to e^+e^-\pi^0$ and $e^+e^- \to e^+e^-\pi\pi$ in space-like kinematics.

2.3. $\pi\pi$ intermediate states

The contribution from $\pi\pi$ intermediate states can be expressed as [8]

$$a_\mu^{\pi\pi} = e^6 \int \frac{d^4q_1}{(2\pi)^4} \int \frac{d^4q_2}{(2\pi)^4} \frac{\sum_i I_i(s, q_1^2, q_2^2) T_i^{\pi\pi}(q_1, q_2; p)}{q_1^2 q_2^2 s Z_1 Z_2}, \tag{3}$$

in a way similar to the pion pole (2). The $T_i^{\pi\pi}(q_1, q_2; p)$ again denote known kinematic functions, while the information on the amplitude on the cut is hidden in the dispersive integrals $I_i(s, q_1^2, q_2^2)$. For instance, the first S-wave term reads

$$\begin{aligned}
I_1\big(s, q_1^2, q_2^2\big) &= \frac{1}{\pi} \int_{4M_\pi^2}^{\infty} \frac{ds'}{s' - s} \bigg[\bigg(\frac{1}{s' - s} - \frac{s' - q_1^2 - q_2^2}{\lambda(s', q_1^2, q_2^2)} \bigg) \\
&\quad \times \operatorname{Im} h^0_{++,++}\big(s'; q_1^2, q_2^2; s, 0\big) \\
&\quad + \frac{2\xi_1\xi_2}{\lambda(s', q_1^2, q_2^2)} \operatorname{Im} h^0_{00,++}\big(s'; q_1^2, q_2^2; s, 0\big) \bigg]
\end{aligned} \tag{4}$$

with Källén function $\lambda(x, y, z) = x^2 + y^2 + z^2 - 2(xy + xz + yz)$, normalization of longitudinal polarization vectors ξ_i, and partial-wave helicity amplitudes $h^J_{\lambda_1\lambda_2,\lambda_3\lambda_4}(s; q_1^2, q_2^2; q_3^2, q_4^2)$ for

$$\gamma^*(q_1, \lambda_1)\gamma^*(q_2, \lambda_2) \to \gamma^*(q_3, \lambda_3)\gamma^*(q_4, \lambda_4) \tag{5}$$

with angular momentum J. By means of partial-wave unitarity

$$\begin{aligned}
&\operatorname{Im} h^J_{\lambda_1\lambda_2,\lambda_3\lambda_4}\big(s; q_1^2, q_2^2; q_3^2, q_4^2\big) \\
&\quad = \frac{\sqrt{1 - 4M_\pi^2/s}}{16\pi} h_{J,\lambda_1\lambda_2}\big(s; q_1^2, q_2^2\big) h_{J,\lambda_3\lambda_4}\big(s; q_3^2, q_4^2\big),
\end{aligned} \tag{6}$$

the imaginary part in (4) is related to the helicity partial waves $h_{J,\lambda_1\lambda_2}(s; q_1^2, q_2^2)$ for $\gamma^*\gamma^* \to \pi\pi$, which have to be determined from experiment.

One key feature in the derivation of (3) concerns the subtraction polynomial. Frequently, dispersion relations need to be subtracted to render the integrals convergent, and the ensuing subtraction constants are free parameters of the approach that need to be determined either from experiment or by further theoretical means, such as effective field theories or lattice QCD. For HLbL scattering, however, gauge invariance puts very stringent constraints on the amplitude and the subtraction polynomial. Therefore, the situation is actually similar to HVP, where the combination of analyticity, unitarity, and gauge invariance provides a parameter-free relation between the contribution to a_μ and the experimental input, the hadronic e^+e^- cross section, as well.

3. Experimental input

By means of a Wick rotation the loop integrals in (2) and (3) can be brought into such a form that only space-like momenta appear in the integral, so that in principle all required information can be extracted from the processes depicted in Fig. 2. However, this would require double-tag measurements for arbitrary negative virtualities, and, in the $\pi\pi$ case, sufficient angular information to perform a partial-wave analysis.